Electronic Supplementary Material (ESI) for Energy & Environmental Science

Supporting Information

Thermoelectric Bi_2Te_3-Improved Charge Collection for High-Performance Dye-Sensitized Solar Cells

Tao Chen, Guan Hong Guai, Cheng Gong, Weihua Hu, Jixin Zhu, Hong Bin Yang, Qingyu Yan and Chang Ming Li

1. Materials and synthesis

Materials: Bismuth citrate (99.99% trace metals basis), sodium telluride (99 %), diethyleneglycol, polyethylene glycol, sodium hydroxide and poly(acrylic acid) (M_w: 1800000) were purchased from Aldrich. Dye sensitizer *cis*-bis(isothiocyanato)(2,2'-bipyridyl-4,4'-dicarboxylato)(2,2'-bipyridyl-4,4'-dinonyl) ruthenium (II) (coded as **Z907**), TiO_2 paste (DSL 18NR-T) and iodide-based liquid electrolyte (HL-HPE) were purchased from Dyesol company. Single-walled carbon nanotube, carbon >90 %, ≥77% (0.7-1.1 nm diameter), and multi-wall carbon nanotube (≥95%, diam. × L = 20-50 nm × 5-20 μm) were also purchased from Aldrich.

Synthesis of Bi_2Te_3: Bi_2Te_3 nanoplates with average edge lengths at 300-400 nm and thickness is 50-80 nm of the Bi_2Te_3 nanoplates were synthesized by a solvothermal method. In detail, 39.88 mg bismuth citrate and 33.74 mg sodium telluride were firstly dissolved in diethylene glycol and polyethylene glycol (15mL/15mL, v/v), followed by adding NaOH (1mL, 5 M) and poly(acrylic acid) (5 mL, 2.5 mg/mL). The mixture was sonicated for 5 min to make a homogenous solution. The solution was thus transferred to autoclave and sealed, heating at 180 ^oC for 8 hrs. After that, the autoclave was cooled down to room temperature. The product was collect by centrifuging at 10 K rpm, 10 min, in a centrifuge tube (50 mL). To further purify the product, ethanol was added to re-disperse the residue. The product was separated again by centrifugation at 10 K rpm, 10min. This purification process was repeated for another 2 times. The black product was finally dissolved in ethanol for use.

2. Supporting Text

2.1 Supporting characterizations

XRD pattern (**Figure S2a**) correspond well with the JCPDS card No. 85-0439 with of hexagonal Bi_2Te_3. **Figure S2d** shows the UV-vis-NIR absorption spectrum of the as-synthesized product. TEM and SEM image shows that the average edge lengths at 150-500 nm and thickness is 20-30 nm of the Bi_2Te_3 nanoplates (**Figure S2e** and **f**). It can also be seen from TEM image that the Bi_2Te_3 nanoplates are porous structure, which could enhance the thermoelectric properties by decreasing the thermal conductivity.[1] The efficiency of converting "waste heat" into useful electricity by thermoelectric materials is usually about 7-8%.[2]

To investigate the composition of the anode, we carried out XRD characterization of the TiO_2 anode. The anode containing either pure TiO_2 nanoparticle or TiO_2/Bi_2Te_3 hybrid nanoparticles were scraped from the FTO surface. XRD pattern (**Figure S2b**) of the anode of device **1** shows an anatase structure of TiO_2 (JCPDS card No. 84-1286). Due to the very small content of Bi_2Te_3 in the TiO_2 electrode, it is difficult to obtain XRD patterns of the Bi_2Te_3 from the hybrid anode in the main text. We thus prepared a film with high amount of Bi_2Te_3 especially for XRD characterization (1/1, w/w). It can be seen that the co-existence of Bi_2Te_3 and TiO_2 (**Figure S2c**).

The cross-section of the anode films were investigated by SEM. For the characterization, the TiO_2 anodes glasses were broken by a hammer. It can be found that Bi_2Te_3 nanoplates can be covered by a dense layer of TiO_2 (**Figure S3a**, from device **3**). At high concentration of Bi_2Te_3 in the TiO_2 paste (**Figure S3b**, from device **4**), Bi_2Te_3 tend to aggregate, which lead to a poor distribution and less "accelerator" loci for electron transport.

2.2 Carbon nanotube incorporated DSCs

Owing to the device temperature increase, one could also expect that the performance increasing in the hybrid Bi_2Te_3-incorporated DSCs is a result of thermal induced better conductivity of Bi_2Te_3. Hence, we employed multi-walled carbon nanotube (MWCNT) to substitute for Bi_2Te_3 to perform similar investigation to device **2**, **3** or **4**; MWCNT is a conductor with very small Seebeck coefficient, 17 $\mu V\ K^{-1}$,[3] it was mixed with TiO_2 commerical paste with weight ratio of 1:4000. Considering the molecular weight of carbon is 1/66.7 of Bi_2Te_3, the amount of MWCNT in the TiO_2 paste is comparable to Bi_2Te_3 in device **3**. The hybrid paste was pasted onto the FTO surface form the bottom layer of the anode.

After incorporation of MWCNT, the J_{sc}, V_{oc} and FF of the hybrid device become 14.52 mA cm^{-2}, 0.69 V and 62 %. The power conversion efficiency was also increased to 6.26 % (the PCE of normal DSC is 6.08 % in this work, see **Table 1** in main text), similar to other reports that the conductivity of MWCNT can improve the performance.[4]4 However, after sunlight illumination, the conversion efficiency of MWCNT-incorporated DSCs gradually decreased from 6.26 % to 6.08 % at 150 min (**Figure S4a**). This observation rules out that the conductivity change of Bi_2Te_3 or MWCNT upon temperature variation can induce better energy conversion efficiency. On the other hand, it is also possible that the Seebeck coefficient of MWCNT is too small (about 1/14 of Bi_2Te_3) to improve the performance that can suppress the inherent deterioration of the DSC.

SWCNT possesses higher Seebeck coefficient, 45 μV K^{-1}, than that of MWCNT (17 μV K^{-1}), but smaller than that of Bi_2Te_3 (240 μV K^{-1}).[3] Therefore, it can be expected that the incorporation of SWCNT into the TiO_2 photoanode could suppress the performance degradation and thus improve the efficiency. **Figure S4b** shows the *J-V* characteristics of the SWCNT-incorporated DSCs. In the SWCNT-incorporated DSC, J_{sc} and η increased to 16.22 mA cm^{-2} and 6.54% compared with the normal DSC. V_{oc} remains unchanged at 0.73 V. Upon sunlight illumination, J_{sc} and η increased gradually and reached their maxima at about 90 min, 16.74 mA cm^{-2} and 6.66 % (**Figure S4**). Although the improvement is very small, this result demonstrates the generality and reliability of utilization of thermoelectric materials for improving the efficiency of the DSCs.

3. Supporting figures

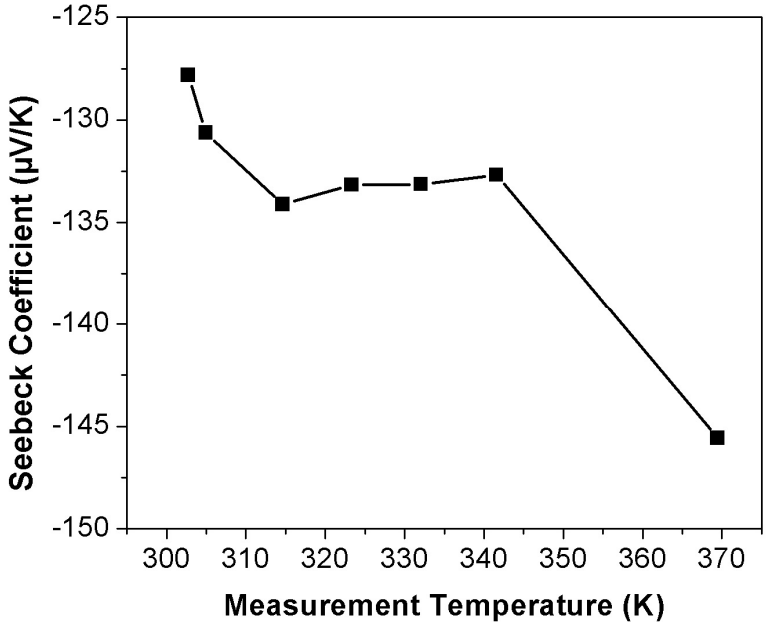

Figure S1. Seebeck coefficients measured on the film sample of Bi_2Te_3 nanoplates in the temperature range of 298-373 K.

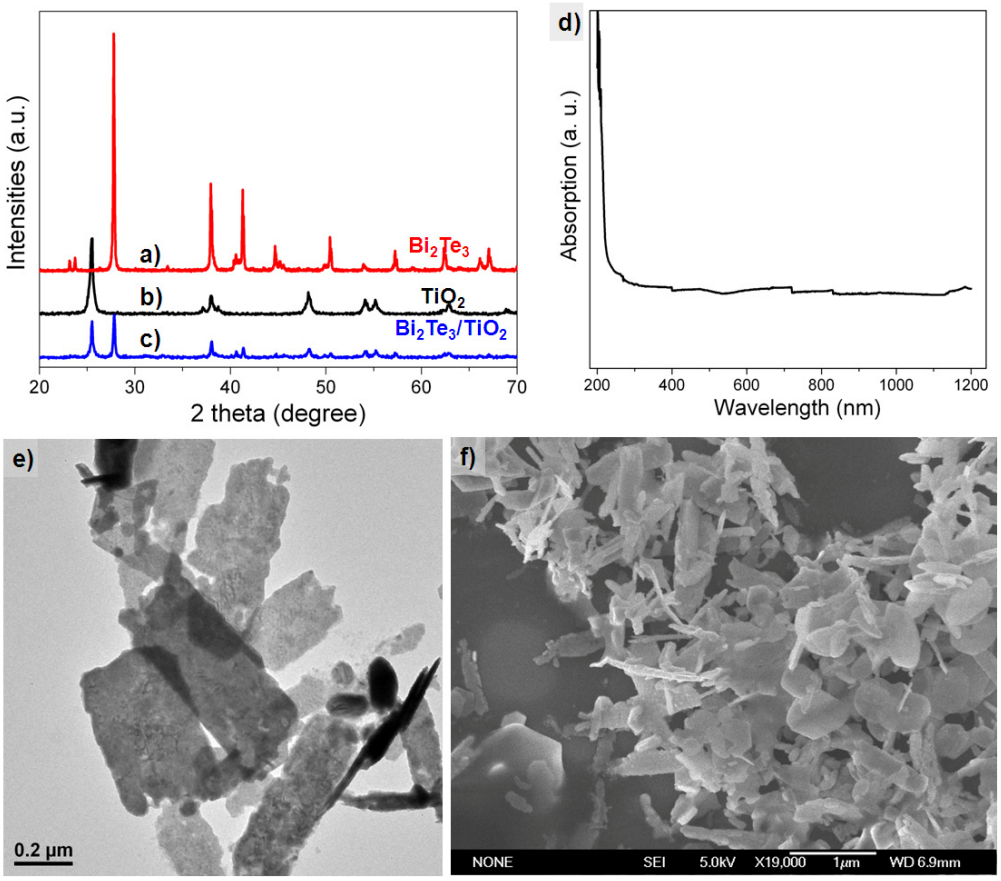

Figure S2. (a), (b) and (c) showing the XRD patterns of Bi_2Te_3, the anode materials of device **1** (TiO_2) and hybrid film of TiO_2/Bi_2Te_3; (d) displaying the UV-vis-NIR absorption of the as-synthesized Bi_2Te_3 nanoplate a. q. solution; (e) and (f) representing TEM and SEM image of the as-synthesized Bi_2Te_3 nanoplates.

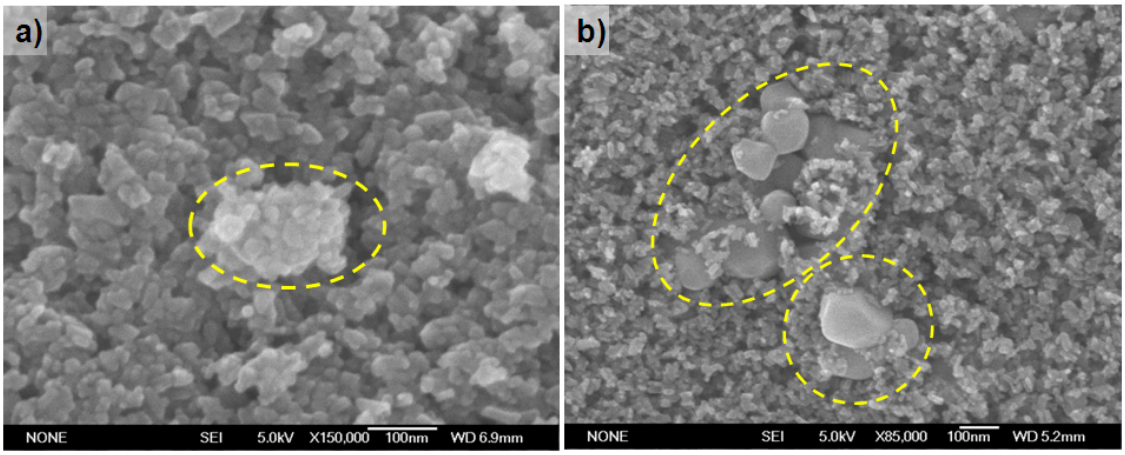

Figure S3. SEM image of cross-section of device **3** (a), Bi_2Te_3 nanoplate was densely decorated by TiO_2 nanoparticles; (b) showing the SEM image of the cross-section of device **4**, there are some aggregates of Bi_2Te_3 due to the high concentration of Bi_2Te_3 nanoplates.

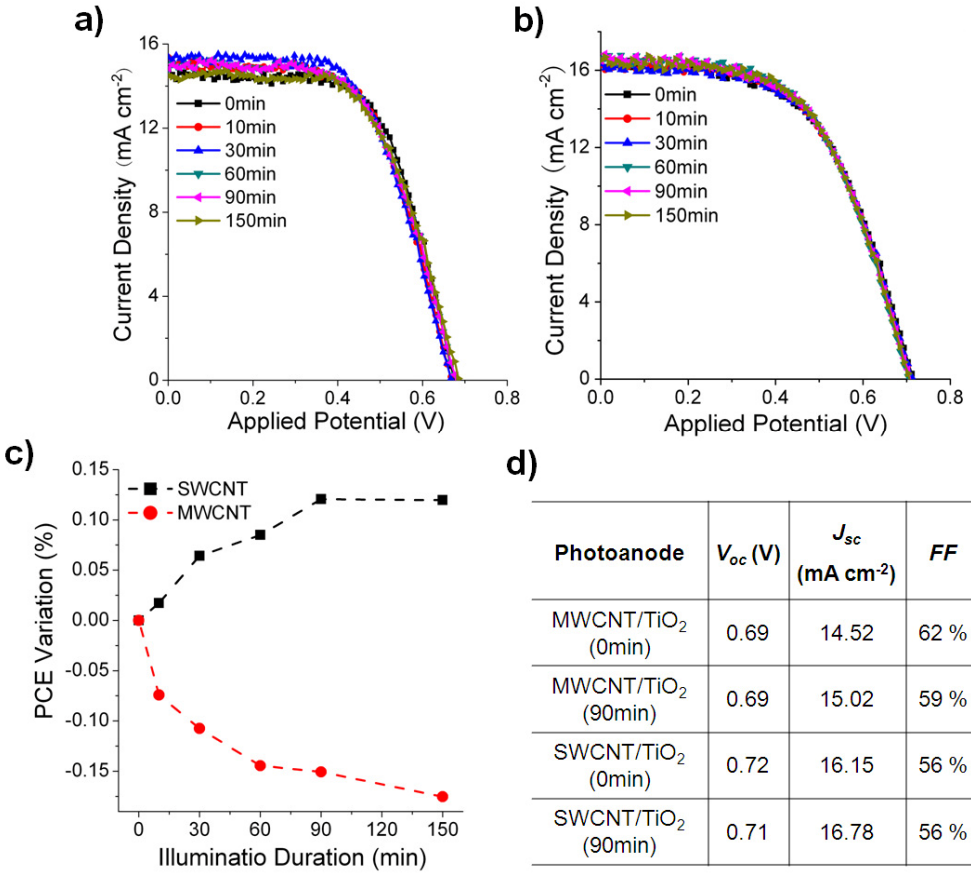

Photoanode	V_{oc} (V)	J_{sc} (mA cm^{-2})	*FF*	*η* (%)
MWCNT/TiO_2 (0min)	0.69	14.52	62 %	6.26
MWCNT/TiO_2 (90min)	0.69	15.02	59 %	6.10
SWCNT/TiO_2 (0min)	0.72	16.15	56 %	6.54
SWCNT/TiO_2 (90min)	0.71	16.78	56 %	6.66

Figure S4. (a) and (b) showing the *J-V* characteristics of the MWCNT- and SWCNT-incorpoarted upon long illumination by sunlight; (c) displaying the PCE variation of the corresponding MWCNT- and SWCNT-incorporated hybrid devices; (d) showing the performance of the MWCNT- and SWCNT-incorporated hybrid devices at 0 min and 90 min sunlight irradiation.

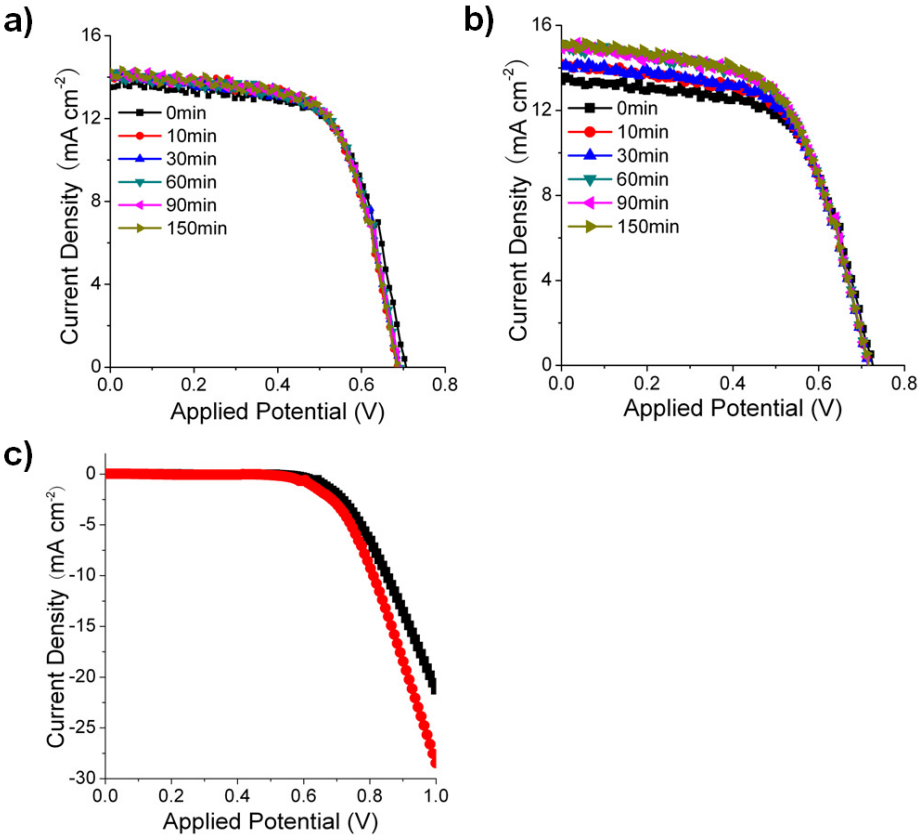

Figure S5. (a) and (b) showing the *J-V* characteristics of device **2** and **4** upon long illumination by sunlight; (c) displaying the *J-V* characteristics of device **4** under dark, it can be seen that after heating by sunlight irradiation, dark current is higher that without long time illumination. Similar to that of device **3** in main text.

4. Supporting References

[1] J. Y. Tang, H. T. Wang, D. H. Lee, M. Fardy, Z. Y. Huo, T. P. Russell, P. D. Yang, *Nano Lett.* **2010**, *10*, 4279.

[2] T. M. Tritt, M. A. Subramanian, *MRS Bull.* **2006**, *31*, 188.

[3] A. M. Rao, X. H. Ji, T. M. Tritt, *MRS Bull.* **2006**, *31*, 218.

[4] S. Muduli, W. Lee, V. Dhas, S. Mujawar, M. Dubey, K. Vijayamohanan, S. H. Han, S. Ogale, *Acs Appl. Mater. & Interfaces* **2009**, *1*, 2030.